BIOCHEMISTRY
including biophysical chemistry & molecular biology

Article

pubs.acs.org/biochemistry

Perturbing the Water Cavity Surrounding the Manganese Cluster by Mutating the Residue D1-Valine 185 Has a Strong Effect on the Water Oxidation Mechanism of Photosystem II

Preston L. Dilbeck, Han Bao, Curtis L. Neveu, and Robert L. Burnap*

Department of Microbiology and Molecular Genetics, Oklahoma State University, 307 Life Sciences East, Stillwater, Oklahoma 74078, United States

Supporting Information

ABSTRACT: The active site of water oxidation in Photosystem II (PSII) is a Mn_4CaO_5 cluster that is located in a cavity between the D1 and CP43 protein subunits by which it is coordinated. The remainder of this cavity is filled with water molecules, which serve as a source of substrate and participate in poorly understood hydrogen bond networks that may modulate the function of the Mn_4CaO_5 cluster. These water molecules interact with the first and second sphere amino acid ligands to the Mn_4CaO_5 cluster and some water interacts directly with the Mn_4CaO_5 cluster. Here, the results of mutations to the amino acids that line the walls of several predicted cavities in the immediate vicinity of the Mn_4CaO_5 cluster were examined in *Synechocystis* sp. PCC 6803. Of these, mutations of Val185 in the D1 subunit resulted in the most interesting functional alterations. The hydrophobic D1-Val185 occupies a location contacting water molecules that are positioned between the redox active tyrosine (Y_Z) and the putative proton gate residue, D1-Asp61, and at a position opposite the oxo bridge atom, O5, of the cluster. Mutations of the residue D1-Val185 were produced, with the intention that the substitute residue would extend into the water cavity that includes H_2O molecules that interact with the Mn_4CaO_5 cluster, amino acid ligands of the Mn_4CaO_5 cluster, Y_Z and the chloride co-factor of PSII. Three of these mutants, D1-Val185Asn, D1-Val185Thr, and D1-Val185Phe, were able to accumulate significant levels of charge separating PSII and were characterized using polarographic and fluorescent techniques. Of the three substitutions, the phenylalanine substitution was the most severe with a complete inability to evolve oxygen, despite being able to accumulate PSII and to undergo stable charge separation. The threonine substitution had no apparent effect on oxygen evolution other than a 40% reduction in the steady state rate of O_2 production compared to the case of wild-type *Synechocystis*, due to a reduced ability to accumulate PSII centers. The asparagine substitution produced the most complex phenotype with respect to O_2 evolution. Although still able to evolve oxygen, D1-Val185Asn does so less efficiently than wild-type PSII, with a higher miss factor than that for the wild type. Most significantly, asparagine substitution dramatically retards the rate of O_2 release and results in an extension of the kinetic lag phase prior to O_2 release that is highly reminiscent of the effects of mutations produced at D1-Asp61. The observed effects of the D1-Val185Phe and D1-Val185Asn mutations may be due to alterations in the environment of nearby chloride co-factor of PSII and/or alterations in the hydrogen bond network, perhaps impeding the movement of water to a binding site on the metal cluster.

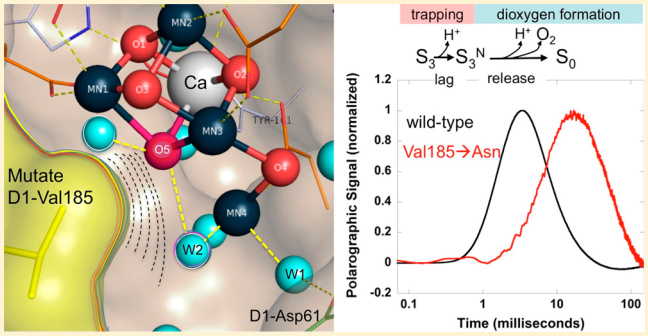

Recently, a three-dimensional model of PSII based on X-ray crystallography was presented, with a resolution of 1.9 Å,[1] a significant improvement on previous models.[2−5] As well as confirming the presence of the metal linking μ-oxo bridges within the Mn_4CaO_5 cluster, this new model also revealed the location of a number of water molecules surrounding the Mn_4CaO_5 cluster, which had previously been unresolved. This includes several apparent water ligands of the Mn_4CaO_5 cluster and others that reside in the previously described water pathways that lead from the Mn_4CaO_5 cluster to the surface of PSII.[6,7] The H_2O broad channel is connected to the narrow channel, which may provide access for substrate water to the Mn_4CaO_5 cluster,[8] but it is also likely to play a role in proton transfer.[9]

To help determine the role of these water channels, a set of point mutations was generated in segments of the water-containing cavities at the interface between D1 and the Mn_4CaO_5 cluster (Figure 1). These are the first mutations constructed to intentionally alter the waters surrounding the manganese cluster. These mutants were characterized in regard to their oxygen evolving and chlorophyll fluorescence properties. Because the selected residues do not act as ligands to the Mn_4CaO_5 cluster, any phenotypes present in these mutants can be presumed to be due to a structural deformation to PSII,

Received: July 13, 2013
Revised: September 6, 2013
Published: September 7, 2013

dx.doi.org/10.1021/bi400930g | *Biochemistry* 2013, 52, 6824−6833

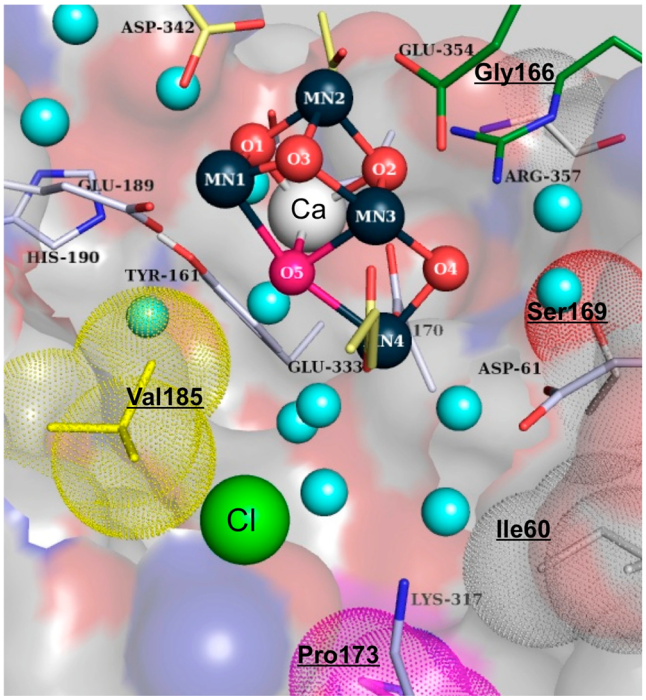

Figure 1. Mutations of the second sphere ligation environment of the Mn_4CaO_5 cluster. One or more single amino acid substitutions were made to the D1 residues D1-Ile60, D1-Gly166, D1-Ser169, D1-Pro173, and D1-Val185. Each of these mutations was produced with the goal of disturbing the water molecules (light blue spheres) surrounding the Mn_4CaO_5 cluster, without disturbing protein folding. The mutants with substitutions to D1-Val185 were found to affect the water oxidation activity of PSII to varying degrees and are the main focus of the present study.

aberrant interactions with substrates or production of the water oxidation reaction, and/or due to the disruption of the H_2O/hydrogen bond network. Although significantly lower levels of PSII accumulation, variable chlorophyll fluorescence and oxygen evolution were observed in the mutants with substitutions to the positions D1-Ile60, D1-Gly166, D1-Ser169, and D1-Pro173 (Table S1 of the Supporting Information); the mutants with substitutions to the residue D1-Val185 were observed to have the most interesting results and were subjected to further characterization.

The side chain of D1-Val185, which is 3.7 Å from the Mn_4CaO_5 cluster, faces the broad channel as it passes the Mn_4CaO_5 cluster (Figure 1). One of these channels, the broad channel, comes into contact with Y_Z, D1-Asp170, D1-Asp61, D2-K317 and one of the chloride binding sites. It also contains many of the H_2O molecules present in the 1.9 Å PSII structure that interact with the Mn_4CaO_5 cluster or its ligands[1] including the H_2O molecules that participate in the hydrogen bond network that is proposed to facilitate the low energy hydrogen bond between Y_Z and D1-His190.[10] Although D1-V185 is not positioned to block the access of substrate water to the Mn_4CaO_5 cluster, mutation of D1-V185 has the potential to alter the interactions of water around the Mn_4CaO_5 cluster notably the essential Cl^- co-factor and the O5 oxygen of the Mn_4CaO_5 cluster. Thus, it is not surprising that mutations at this location can produce dramatic changes in the kinetics of water oxidation the Mn_4CaO_5 cluster as described below.

METHODS AND MATERIALS

Strains and Growth Conditions. The naturally transformable, glucose-utilizing strain of *Synechocystis* sp. PCC 6803 and the mutant derivatives were maintained on solid agar and in liquid blue-green-11 (BG-11) medium buffered with 20 mM 4-(2-hydroxyethyl)-1-piperazineethanesulfonic acid (HEPES)−NaOH (pH 8.0) (HBG-11) supplemented with 5 mM glucose and 10 μM 3-(3,4-dichlorophenyl)-1,1-dimethylurea (DCMU).[11−16] Experimental cultures were inoculated from solid media into 100 mL of HBG-11 with 5 mM glucose and grown while shaking under a photon flux density of ∼80 μM m^{-2} s^{-1} at 30 °C. Light intensity measurements were made with a Walz universal light meter 500 (Effeltrich, Germany). All mutants were constructed in the *psbA2* gene and introduced to a recipient strain of *Synechocystis* lacking all three *psbA* genes and contained a hexahistidine "tag" genetically fused to the C-terminus of the CP47 protein.[16−18] A hexahistidine-tagged control strain was similarly constructed using the same *psbA*-less recipient strain, but transformed with the wild-type *psbA2* gene resulting in a strain possessing PSII activity similar to that of the true wild type[19,20] and is referred to as the wild type.

Isolation of Thylakoid Membranes. Thylakoid membranes were isolated essentially as before.[11,14,15] *Synechocystis* cells were grown to mid-log phase and then harvested by centrifugation for 10 min at 8000*g* and then resuspended in 50 mM 2-(*N*-morpholino)ethanesulfonic acid (MES)−NaOH (pH 6.0), 10% glycerol (v/v), 1.2 M betaine, 5 mM $MgCl_2$, and 5 mM $CaCl_2$ to a concentration of 1 mg of chlorophyll mL^{-1}. The resuspended cells were incubated in the dark and on ice for 1 h. Prior to cell breakage, benzamidine, ε-amino-η-caproic acid, and phenylmethanesufonyl fluoride were added to the cell suspension at a concentration of 1 mM each. The cells were broken by five cycles (5 s on and 5 min off) of agitation with 0.1 mm diameter zirconium/silica beads in a Bead-Beater (BioSpec Products, Bartlesville, OK, USA). The extracted thylakoid membranes were collected by centrifugation at 14 000 rpm for 30 min at 4 °C in a tabletop centrifuge (Eppendorf 5417R, Hauppauge, NY, USA). The pelleted thylakoid membranes were resuspended in 50 mM MES−NaOH (pH 6.0), 10% glycerol (v/v), 1.2 M betaine, 20 mM $CaCl_2$, and 5 mM $MgCl_2$ to a Chl concentration of 1−1.5 mg mL^{-1}, before being flash-frozen in liquid nitrogen and stored at −80 °C.

Polarographic Measurements of O_2 Evolution. Measurements of flash number dependent O_2 yields and O_2 release kinetics were performed with isolated thylakoid membranes using a bare platinum electrode that allows for the deposition of samples by centrifugation as described previously.[13,21−23] For each measurement, a sample of thylakoid membranes containing 3 μg of chlorophyll was added to 500 μL of 50 mM MES−NaOH (pH 6.5), 1 M sucrose, 200 mM NaCl and 10 mM $CaCl_2$. Samples were centrifuged onto the electrode surface at 8000*g* for 10 min at 25 °C in a Sorvall HB-4 swing out rotor. The temperature of the electrode was regulated by circulating thermostated water through a copper jacket that surrounds the electrode. Polarization of the electrode (0.73 V) was turned on 20 s before the start of data acquisition, and the flash sequence was started 333 ms after that. The response time of the polarographic amplifier is approximately 100 μs, whereas the electrode−electrolyte system responds within approximately 200−400 μs at the specified NaCl concentration in the measuring buffer. Acquisition of the data and the control of the instrumentation was implemented using a plug-in data

dx.doi.org/10.1021/bi400930g | *Biochemistry* 2013, 52, 6824−6833

acquisition circuitry and LabView software (National Instruments, Austin, Texas) that permitted timing and coordination of the flash illumination and data acquisition in a synchronous mode with nanosecond accuracy (independent of computer motherboard and operating system). Timing of the flash points relative to the O_2 signals and instrument response time was verified in separate trials by observing the photoelectric signal resulting from exposing the silver electrode to unfiltered xenon flashes. Samples were allowed to thermally equilibrate to the temperature of the water jacket for 10 min on the electrode receiver before the data acquisition was initiated. This proved critical in obtaining reproducible oxygen signal decay transients due to their strong temperature dependence especially seen in the rate of the decay of O_2 signal. Samples were exposed to a train of 50 μs flashes from a red (nominally 627 nm) Luxeon III emitter light-emitting diode (LED) (Philips Electronics, Amsterdam) driven by a strobe current generator (Pulsar 710, Advanced Illumination, Rochester, VT, USA), placed 0.9 cm from the surface of the electrode given at 2 Hz after allowing the sample and electrode to temperature equilibrate to 30 °C. Each sample was exposed to up to 720 flashes, and the signals were averaged.

Steady State Rates of Oxygen Production. Steady state rates of oxygen evolution from whole cells were measured using a Clark electrode.[24] Measurements were made using samples containing 10 μg of Chl taken from cells suspended in a HN buffer [10 mM HEPES−NaOH and 30 mM NaCl (pH 7.0)]. The samples were exposed to a saturating light in the presence of 2 mM $K_3Fe(CN)_6$ and 750 μM DCBQ for 60 s. The maximal O_2 rates were calculated from the segment of the O_2 concentration trace with the greatest slope and averaged from the results of three measurements.

Quantification of PSII and Measurements of Fluorescence Kinetics. Measurements of variable fluorescence yields were performed with a double-modulation kinetic chlorophyll fluorometer fitted with a second actinic flash illumination source (PSI Instruments, Brno, Czech Republic). Cells from the mid-log growth phase were kept under dim light on a shaker at 200 rpm before being used for experiments and diluted to 5 μg of Chl/mL for measurements. Fluorescence kinetics were assayed using variations of the standard instrument settings that sample the low-fluorescence F_0 state in dark-adapted samples by probing fluorescence yield with four measuring pulses followed 200 μs later by a 30 μs saturating actinic flash, followed by a sequence of measuring pulses beginning 50 μs after the actinic flash. PSII has a high fluorescent yield when it is in the $P680Q_A^-$ state, which is formed when P680 absorbs a photon of light and donates an electron to Q_A. Without inhibitors, the principal component of the decay of this state is due to the oxidation of Q_A^- by a plastoquinone in the Q_B site. When DCMU blocks the transfer of electrons from Q_A to Q_B, this causes $P680Q_A^-$ to persist until the electron recombines with oxidants on the donor side, which in the case of the intact enzyme is principally the S_2 state of the Mn_4CaO_5 cluster. The total variable fluorescence was evaluated with the equation $F_v = (F_t - F_0)/F_0$, where F_t is the fluorescence at time t and F_0 is the lowest level of fluorescence yield obtained as the average yield of a sequence of four weak measuring flashes applied before the first saturation flash. Analysis of the kinetic components of the fluorescence decay was performed according to Allahverdiyeva et al., except that a correction for exciton sharing between centers was not applied.[25,26]

Estimation of the concentration of charge-separating PSII centers was performed essentially as described previously.[23,27] The cells were incubated in the dark for 5 min with 300 μM dichlorobenzoquinone (DCBQ) and 300 μM $K_3Fe(CN)_6$ to oxidize any residual Q_A^-. DCMU was then added at a concentration of 20 μM, the mixture was allowed to incubate for 1 min, and then 10 mM hydroxylamine was added. Measurement of variable fluorescence was initiated several seconds after the hydroxylamine was added by applying 30 saturating actinic flashes (20 Hz), with the fluorescence yield being sampled after each flash.

RESULTS

Mutagenesis. Several amino acids on the D1 subunit of PSII were targeted for mutagenesis on the basis that their side chains face the water cavity surrounding the Mn_4CaO_5 cluster (Figure 1). Sites for possible mutation were discovered by analyzing the crystal structure of PSII for unoccupied spaces in the crystal structure that are large enough to accommodate water molecules. This was accomplished using PyMOL in conjunction with the cavity finding algorithm Caver[28] to identify channels in the 2AXT PSII structure.[4] These cavities were largely in agreement with the channels previously described by Ho and Styring[7] and, to a lesser extent, those described by Murray and Barber.[6] Indeed, after the initial design and construction of the mutants, the high-resolution structure of the PSII complex with water molecules was determined[1] and these cavities in the proteins structure were shown to be occupied by water. The amino acid residues chosen for mutagenesis were D1-Ile60, D1-Gly166, D1-Ser169, D1-Pro173, and D1-Val185. One or more point mutations were constructed in *Synechocystis* at each of these amino acid sites with the goal of occupying space inside PSII that is normally occupied by water or to change the interaction between the cavity surface with that water so as to allow, for example, aberrant hydrogen bond interactions (Figure 1).

Each mutant was assayed for its ability (1) to grow photoautotrophically, (2) to accumulate PSII, (3) to undergo stable charge separation, and (4) to produce O_2. The purpose of these tests was to determine whether each point mutation was detrimental to photosynthetic water oxidation and, if so, whether this was due to a defect in the water-oxidation mechanism or due to an inability to assemble stable PSII complexes. Because the aim is to help provide an understanding of the role of the surrounding water in facilitating the water-oxidation mechanism, the most interesting mutants will allow assembly of PSII complexes yet alter the catalytic properties of the Mn_4CaO_5 cluster. Photoautotrophic growth was assayed by inoculation onto solid BG-11 growth media and incubation in standard growth conditions, and steady state maximal rates of O_2 production were measured using a Clark-type electrode (Table 1 and Table S1 of the Supporting Information).

The ability of each strain to assemble the Mn_4CaO_5 cluster in PSII and to undergo a stable charge separation was assayed using a dual modulation kinetic fluorometer. The change in the yield of variable chlorophyll fluorescence $(F_t - F_0)/F_0$ induced by a single saturating flash in the presence of DCMU is proportional to the fraction of PSII centers present in each sample that are able to form the $P680Q_A^-$ state (which has a higher fluorescence yield than the $P680Q_A$ state) in response to the saturating flash. As discussed below, the decay of the high fluorescence state, in part, reflects the characteristics of the donor side of the PSII complex including whether it is capable

Table 1. Characterization of Wild Type and D1-V185 Mutant Strains of *Synechocystis* sp. PCC 6803

strain	photoautotrophic growth	relative PSII content (% of wt)[a]	F_v (% of wt)[b]	oxygen evolution (% of wt)[c]
wild type	+	100	100	100
D1-V185F	−	96	56	0
D1-V185D	−	ND[d]	ND	ND
D1-V185N	+	83	71	41
D1-V185T	+	76	61	60
D1-V185W	−	16	10	0

[a]The relative PSII content of each strain was estimated from the yield of variable chlorophyll a fluorescence $(F_{max} - F_0)/F_0$ after 40 flashes. Measurements were taken in the presence of 20 mM hydroxylamine and 20 μM DCMU, according to previously described methods.[23,27] [b]The ability of each strain to undergo a stable charge separation was assessed by recording the yield of variable fluorescence $(F_{max} - F_0)/F_0$ after a single actinic flash in the presence of 20 μM DCMU. [c]Steady state rates of oxygen evolution were measured with a Clark-type electrode using a chlorophyll concentration of 6.35 μg in HN buffer [10 mM HEPES−NaOH and 30 mM NaCl (pH 6.5)] with the addition of 750 μM DCBQ and 2 mM K3Fe(CN). Each value represents the average of three or more samples. Standard deviations were less than 20%. [d]ND = not detected using described assays.

of forming the S_2 state of the Mn_4CaO_5 cluster. Thus, it is a good indicator of whether mutant PSII centers are capable of assembling a functional Mn_4CaO_5 cluster. A similar technique was also used to estimate the amount of charge-separating PSII in each mutant culture relative to the wild type. This was done by exposing samples to multiple saturating flashes in the presence of hydroxylamine (HA), a reductant capable of removing the Mn_4CaO_5 cluster and then acting as the electron donor to Y_Z^+.[23,27,29] The presence of DCMU blocking forward electron transfer from Q_A to Q_B, the presence of HA as a donor-side reductant, and multiple saturating flashes ensure that each PSII center is able to reach the high fluorescence yield state, regardless of defects to the water oxidation complex, and therefore it provides a good biophysical measure of relative PSII concentration that compares well with biochemical methods.[27]

Using these fluorescence techniques, we observed several of the D1-Val185 mutant strains accumulate PSII significant concentrations compared to the case of wild-type *Synechocystis*, yet were defective in O_2 evolution. As shown in Table S1 of the Supporting Information, other mutations of residues lining the water cavities near the Mn_4CaO_5 cluster also proved to be of interest based on the above criteria but did not exhibit as strong a negative impact on the water-oxidation complex. The initial characterization of these strains possessing substitutions to D1-Ile60, D1-Gly166, D1-Ser169, and D1-Pro173 can be found in Table S1 of the Supporting Information.

Photosystem II Accumulation and Activity in D1-Val185 Mutant Strains. Five mutant strains were created with single amino acid substitutions of the residue D1-Val185, which faces the broad channel.[7] Two of these, the aspartate (V185D) and tryptophan (V185W) substitutions did not accumulate significant levels of PSII, as evidenced by the lack of a variable fluorescence signal even in the presence of the artificial electron donor, HA. These two strains are likely to be defective in assembling stable reaction center complexes capable of charge separation, as seen with some other PSII mutations.[23,27,29] On the other hand, the mutants with phenylalanine (D1-V185F), asparagine (D1-V185N), and threonine (D1-V185T) substitutions to D1-Val185 were able to accumulate PSII at 96, 83, and 76% of the wild-type level, respectively. Of the three V185 mutants that were able to accumulate PSII, only the D1-V185N and D1-D1-V185T were able to grow photoautotrophically. The lack of autotrophic growth in the D1-V185F mutant is likely due to an inability to evolve oxygen, because only negligible rates of O_2 evolving activity were detected by the Clarke-type electrode (Table 1). The D1-V185N and D1-V185T strains were, on the other hand, able to achieve significant maximal rates of O_2 evolving activity, at 41 and 60% of the wild-type value, respectively.

Fluorescence Decay Kinetics. The kinetics of the relaxation of the chlorophyll fluorescence yield were examined using a dual modulation kinetic fluorometer to examine the properties of the donor and acceptor side electron transfer reactions in PSII. The measurements were taken using dark-adapted cells that had been grown to mid-log phase conditions that ensure maximal PSII activity in these mutants (data not shown). Samples were exposed to a single saturating flash and then a series of weaker measuring flashes. Comparing the fluorescence yield after each measuring flash to a baseline measured before the actinic flash is given allows the calculation of the fraction of PSII centers in the high fluorescence yield

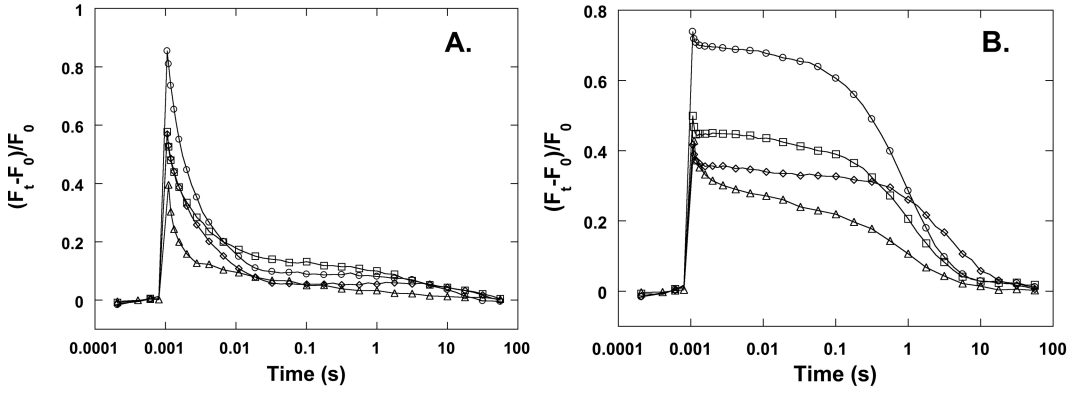

Figure 2. Q_A reoxidation kinetics. The decay kinetics of the flash-induced variable chlorophyll *a* fluorescence $(F_t - F_0)/F_0$ for wild type (circles), D1-V185F (triangles), D1-V185T (diamonds), and D1-V185N (squares) strains of *Synechocystis* were measured in both the absence (panel A) and presence (panel B) of 20 μM DCMU. F_0 was defied as the average fluorescence yield from four weak measuring pulses given to the samples at 200 μs intervals before the exposure of the samples to a 30 μs actinic flash. The actinic flash is followed by a series of weak measuring flashes that monitor the decay of the high fluorescence yield state. See Table S2 of the Supporting Information for the numerical fits of these decay curves.

dx.doi.org/10.1021/bi400930g | *Biochemistry* 2013, 52, 6824−6833

state ($P680Q_A^-$) to the fraction in the low yield fluorescent states ($P680Q_A$ and $P680^+Q_A^-$) to be monitored as the high fluorescent state decays.[30,31] These decay kinetics give information about the electron transfer processes in each strain.

The kinetics of Q_A reoxidation were measured in the wild type, D1-V185F, D1-V185N, and D1-V185T strains of *Synechocystis* in both the presence and absence of DCMU, which is an electron transport inhibitor that blocks the forward movement of electrons from Q_A to Q_B. To analyze the decay kinetics, the fluorescence yield signals were fitted with two functions. For no DCMU signals, the fitting function was composed of two exponential components and one hyperbolic component according to Vass et al.[32] The fast phase is related to reoxidation of Q_A^- by Q_B. The middle phase corresponds to Q_A^- reoxidation in centers with empty Q_B sites at the time of the flash and has to bind a PQ molecule from the PQ pool. The slow phase reflects reoxidation of the Q_A^- or Q_B via a reverse reaction with the S_2 state. When the Q_B site was blocked by DCMU, the decay kinetics was fitted with two phases: the slow phase reflects the Q_A^- reoxidation with the S_2 state, and the fast phase corresponds to the reoxidation of Q_A^- with electron donors that are less stable than the S_2 state. Out of the three mutants that were examined extensively, the Q_A^- reoxidation kinetics of the D1-V185N mutant was the most similar to that of the wild type. Forward electron transfer from Q_A^- to Q_B appears largely unaffected in the D1-V185N mutant as indicated by the similar fluorescence decay kinetics in the absence of DCMU compare to the wild type. In the presence of DCMU the S_2 state and Q_A^- recombined with a $t_{1/2}$ of 860 ms (Table S2 of the Supporting Information). This is slightly slower than the $t_{1/2}$ of 690 ms observed in the wild-type strain (Table S2 of the Supporting Information). This may indicate that the S_2 state of the Mn_4CaO_5 clusters in the D1-V185N mutant have a slightly lower redox potential than in wild-type PSII.

In the D1-V185T mutant there were more substantial differences in the kinetics of Q_A^- reoxidation (Figure 2). The rate of charge recombination between S_2 and Q_A^- was slowed to a $t_{1/2}$ of 2.80 s in the presence of DCMU (Table S2 of the Supporting Information). This again can be interpreted to indicate that the S_2 state of the Mn_4CaO_5 clusters in the D1-V185T mutant have a significantly lower redox potential than in wild-type PSII. The D1-V185T strain also differed from the wild type in the relative contributions of the various charge recombination pathways. This can be determined by comparing the relative amplitudes of each component of the fluorescence decay curve.[25] In this case 89.8% of Q_A^- charge recombination can be attributed to recombination with the Mn_4CaO_5 cluster in the S_2 state and 10.2% can be attributed to other pathways (Figure 2). For comparison, recombination between Q_A^- and the S_2 state accounts for 97.3% of total charge recombination in wild-type *Synechocystis* and 94.1% in the D1-V185N mutant (Table S2 of the Supporting Informaiton).

On the basis of their rates of charge recombination between S_2 and Q_A^-, both the D1-V185T and D1-V185N substitutions appear to lower the S_2/S_1 redox potential of the Mn_4CaO_5 cluster, with the D1-V185T being much more significantly altered. This is a reasonable consequence of replacing a nonpolar residue with polar residues in close proximity to a redox active co-factor. The Mn_4CaO_5 cluster in particular depends on several negatively charged ligands to neutralize the positive charges of the metal ions. In other cases where a second sphere ligand has been replaced by a less electronegative side chain, such as the substitution of D1-Asp61 with asparagine, the rate of charge recombination between S_2 and Q_A^- has been observed to be more rapid than that for the wild type.[33] However, this generalization does not hold true for every amino acid substitution made near the Mn_4CaO_5 cluster.[27,33−35] Other means of affecting the rate of charge recombination between S_2 and Q_A^- should also be considered, especially for substitutions such as the D1-V185 substitutions, which may affect the environment around Y_Z, perhaps via the interconnecting hydrogen bond network leading from Y_Z past the D1-V185 location toward D1-D61. Altering the hydrogen bond network around Y_Z should be expected to alter its redox potential, which also plays a role in the rate of charge recombination between S_2 and Q_A^-. What effect, if any, this should have on the catalytic properties of the Mn_4CaO_5 cluster, in terms of its ability to oxidize H_2O, is unclear.

There were also differences in the amplitudes of the maximum variable fluorescence signals of each mutant (Figure 2). This indicates that the V185 mutants are, to varying degrees, unable to form stable charge separations as efficiently as wild-type PSII. This may be due to less efficient formation of the S_2 state, which is required to stabilize the $Y_ZP680Q_A^-$ state, but the lower levels of PSII content are likely to also play a role, especially in the D1-V185T mutant as evidenced by the assay for concentration of charge-separating centers using HA showing a 40% drop in the accumulation of PSII in the D1-V185T mutant (Table1).

The D1-V185F mutant has substantially altered Q_A^- reoxidation properties compared to those of the wild type. It appears to have a large fraction of centers characterized by rapid rates of charge recombination even in the presence of DCMU (Figure 2). A larger fraction of centers exhibiting rapid decay are also seen in the absence of DCMU (Figure 2, Table S2 of the Supporting Information), indicative of a larger number of centers failing to establish a stable charge separation through the transfer of the oxidant to Mn, but instead only oxidizing Y_Z, which recombines more rapidly with electrons on the acceptor side. This may reflect a subpopulation of PSII centers in the mutant that lack assembled manganese clusters and hence only are capable of storing the charge-separated oxidant as Y_Z^{OX}, which more rapidly recombines with electrons on the acceptor side. However, the D1-V185F nevertheless contains a substantial fraction (~60%) of centers that exhibit a 690 ms decay component similar to the wild-type (Table S2 of the Supporting Information, bottom numerical fits) suggesting that these centers may assemble Mn clusters. However, given the fact that this mutant fails to evolve O_2, it would appear that either (1) the Mn-cluster is not normally assembled despite being capable of storing oxidant with stability properties similar to those of the normal S_2 state or (2) the mutant assembles Mn_4CaO_5 clusters, but the bulky phenylalanine substitution sterically interferes with the waters crucial for advancement through the S state cycle.

S State Cycling and O_2 Release Kinetics. Thylakoid membranes were prepared from each of the V185 mutant strains of *Synechocystis* to further characterize their oxygen evolving activity. The oxygen evolving characteristics of these membranes were analyzed using a bare platinum electrode to determine their S state cycling parameters and rates of O_2 release.[13,36] Measurements taken with the bare platinum electrode confirmed the absence of oxygen evolving activity in D1-V185F PSII centers. The only kinetic feature revealed by exposing centrifugally deposited samples of D1-V185F

dx.doi.org/10.1021/bi400930g | *Biochemistry* 2013, 52, 6824−6833

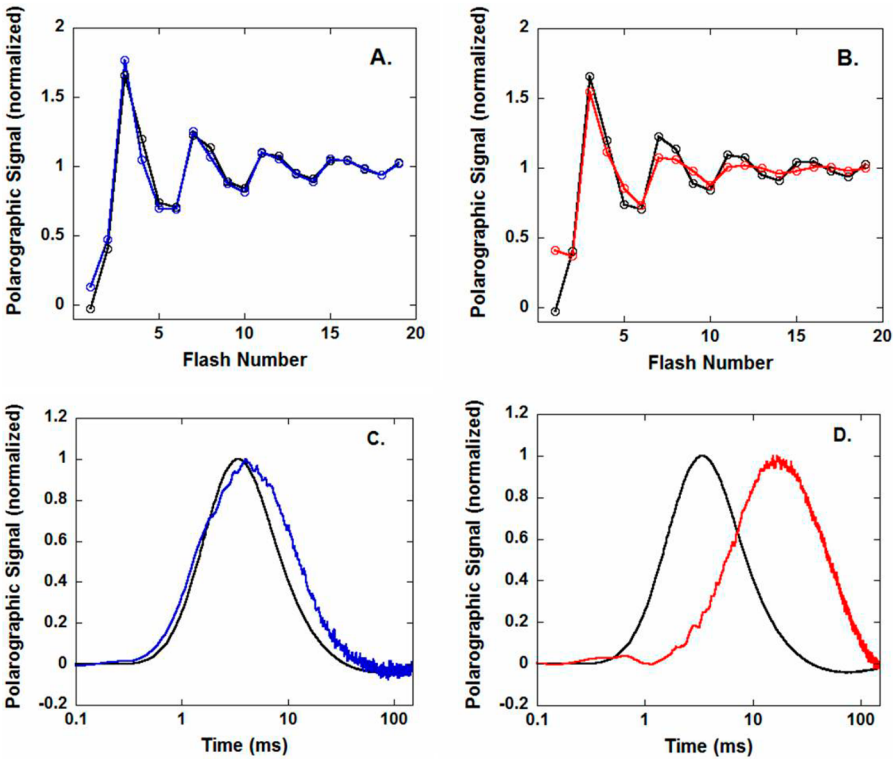

Figure 3. Flash dependent O_2 yields (panels A and B) from wild type (black), D1-V185T (blue), and D1-V185N (red) thylakoid membranes. The signals were normalized to the average amplitude of the last four flashes. Each trace represents the averaged amplitudes from three samples. Panels C and D show the O_2 release signals from wild type (black), D1-V185T (blue), and D1-V185N (red) thylakoid membranes. For O_2 release measurements thylakoid membrane samples containing 3 μg of Chl were centrifugally deposited on to a bare platinum electrode and exposed to a series of measuring flashes from a red LED at 4 Hz. Each trace represents the average of 720 (wild type and D1-V185T) or 1200 (D1-V185N) flashes. For the measurement of the mutant samples the gain of the polarographic amplifier was set to double the sensitivity used to measure the wild type sample.

thylakoid membranes to flashing light was the photoelectric artifact caused by the exposure of the polarized electrode surface to LED pulses. This evidence confirms that D1-V185F mutant strain is unable to evolve oxygen.

The flash dependent O_2 yields of both the D1-V185N and the D1-V185T thylakoid membranes displayed period four oscillation with a peak on the third flash in dark adapted samples exposed to a series of saturating xenon flashes (Figure 3). The S state parameters of the D1-V185T mutant were similar to those of the wild type with only 13% in the miss factor, α (Table 2). The D1-V185N mutant displayed a slightly increased miss factor of 18% compared to the 14% miss factor in the wild-type thylakoid membranes (Table 2).

The O_2 release kinetics observed from D1-V185T thylakoid membranes with the bare platinum electrode were only slightly slower than the O_2 release kinetics of the wild type. The rise kinetics of the D1-V185T O_2 release had a $t_{1/2}$ of 1.5 ms (Table 2), which is only slightly slower than the 1.2 ms $t_{1/2}$, which is characteristic of wild-type PSII in optimal conditions. Unlike the D1-V185T mutant, thylakoid membranes derived from the D1-V185N mutant released O_2 at a substantially slower rate than did the wild-type thylakoid membranes (Figure 3D). These thylakoid membranes also displayed a delayed onset in the release of O_2 after each actinic flash. The combination of a decreased rate of O_2 release and a longer lag phase has also been observed in PSII samples derived from the D61N[36,39,40] mutant strain of *Synechocystis*, in PSII samples where the chloride ion had been replaced by iodide,[41] and in mutations of the chloride ligand D2-Lysine317.[42] However, the lag in the D1-V185N mutant is truly remarkable, being much longer than any mutant studied to date, as analyzed below. The D1-V185N mutant also shares a slightly increased miss factor (Figure 3B, Table 2) with the D61N and iodide substituted PSII samples.[36,41] The relatively higher signal on the flash one is consistent with a dark stable S_3 state in the D1-V185N mutant, yet this conclusion remains very tentative until further analysis is performed, and it is possible that other photoproducts such as hydrogen peroxide production could also produce this initial signal. The role of the chloride ion has been hypothesized to include the modulation of the hydrogen bond network around

Table 2. S State Cycling Parameters of D1-V185 Mutants[a]

strain	S state distribution $S_0/S_1/S_2/S_3$ (%)	misses, α (%)	hits, β (%)	double hits, γ (%)	O_2 signal rise, $t_{1/2}$ (ms)[b]
wild type	24/64/12/0	14	84	2	1.2
D1-V185N	16/80/0/4	18	80	2	27.0
D1-V185T	17/69/13/1	13	85	2	1.5

[a]Thylakoid membranes samples containing 3 μg of Chl exposed to a constant light source for 30 s and then centrifugally deposited on to a bare platinum electrode. The samples were then exposed to a single actinic flash and then dark adapted for 10 min. The flash dependent O_2 yields were then measured from a series of 20 actinic flashes from a xenon flash lamp given at 2 Hz. Estimation of S state parameters was performed using a four-state model as previously described.[22,37] [b]The rate of O_2 release as determined by a previously described mathematical model.[36]

dx.doi.org/10.1021/bi400930g | *Biochemistry* 2013, 52, 6824−6833

D1-Asp61.[43] Because the substitute asparagine residue in the D1-V185N mutant is sufficiently long to interact with the chloride ion, it is possible that the phenotype of these three types of PSII center share a common mechanistic explanation involving D1-Asp61 and its role in the removal of protons from PSII.

To more accurately compare the kinetics of O_2 release from the D1-V185N and D1-D61N mutants, the O_2 release signal collected from the D1-V185N mutant was fit according to a mathematical model of O_2 release that had previously been used to analyze the D61N mutant.[36] This model, developed by Ivelina Zaharieva and Holger Dau,[36] includes components that take into account the diffusion and consumption processes that cause the decay of the polarographic O_2 signal, as well as two rise components corresponding to the resolvable advancement phases of the S_3 to S_0 transition, to more accurately reflect the phenomena that underlie the observed O_2 release signal.[36] The rate of O_2 release estimated by the model for the D1-V185N mutant was 26 ms, which is slightly slower than the 24 ms $t_{1/2}$ observed in the D61N mutant under similar conditions.[36] On the other hand, the lag phase of observed in the D1-V185N signal was slower than the lag phase observed in the D61N mutant at this pH 6.5 condition (0.8 ms versus 0.60 ms).

DISCUSSION

The substitutions to D1-Val185 that were generated for this work represent the first time that point mutations to PSII have been explicitly designed to interfere with the water cavities surrounding the Mn_4CaO_5 cluster. Although a number of other different amino acids were targeted for mutation (Table S1 of the Supporting Information), we focused on the D1-Val185 substitution mutants. Obviously only a small number of possible sites were targeted, but it now seems likely that other sites will also prove interesting regarding the water channels, keeping in mind that a much more highly resolved crystal structure is now available,[1] and more comprehensive modeling of water movement has been performed[7,8,44] since the present set of mutations was first envisaged. Of the D1-V185 mutants, the asparagine (D1-V185N) and phenylalanine (D1-V185F) proved to have dramatic and interesting impacts upon the ability of PSII to evolve oxygen. Although the threonine mutant (D1-V185T) appears to cause a problem with the assembly and/or stability of the PSII complex, the centers that are assembled in the D1-V185T mutant have the least severe phenotype with respect to the intrinsic H_2O-oxidation process (Table 1). The chemical structures of valine and threonine are roughly comparable in size and shape, with the threonine side chain occupying a smaller volume, but having the polar oxygen atom of the hydroxyl group. Analysis of O_2 release by D1-V185T thylakoid membranes with a bare platinum electrode revealed O_2 release kinetics and S state cycling parameters that were nearly identical to those of wild-type thylakoid membranes. The steady state rate of O_2 production by the D1-V185T strain of *Synechocystis* is reduced compared to that of wild-type *Synechocystis*, but this rate is roughly proportional to the number of charge separating PSII centers by the D1-V185T mutant. It is therefore reasonable to assume that the reduced rate of O_2 release from D1-V185T *Synechocystis* is attributable to a reduced ability to assemble active PSII centers, yet the turnover time of the catalytic cycle is not much altered.

Like the D1-V185T mutant, the D1-V185N mutant retained an ability to evolve oxygen (Table 1). However, although there is only a small discrepancy between the ability of D1-V185T to assemble PSII and its ability to evolve oxygen, the D1-V185N mutant can only evolve O_2 at 41% of the rate of the wild type despite being able to accumulate 83% as much PSII. Although the D1-V185T mutant is nearly identical to the wild type in terms of its O_2 release kinetics and S state cycling parameters, the D1-V185N strain displayed clear differences in both (Figure 3B,D). The kinetics of O_2 release from D1-V185N thylakoid membranes were substantially delayed compared to O_2 release from the wild-type thylakoid membranes (Figure 3D). The D1-V185N mutant also displayed a substantial lag period prior to the onset of O_2 release (Figure 3D). In fact, this 0.8 ms lag is the longest lag phase yet recorded in any mutant under similar buffer and temperature conditions. This lag phase is believed to represent the formation of an intermediate in the S_3 to S_0 transition due to the release of a proton triggered by the oxidation of the $Y_Z^{\bullet}$.[45−47] The length of this lag phase in wild-type PSII has typically been observed to be between 50 and 250 μs using various techniques.[45−49] Currently, the observation of the lag phase in wild-type thylakoid membranes is limited by the response time of the available bare platinum electrode and the onset of O_2 release is not observed until 350 μs after the actinic flash.

The phenotype of the D1-V185N mutant is similar to the phenotype of the D1-D61N mutant, another PSII point mutation that has been well characterized.[36,39,40,50] D1-Asp61 is a second sphere ligand of the Mn_4CaO_5 cluster that interacts with substrate water[1,43,51] and is hypothesized to act as the first proton acceptor in the proton exit pathway.[2,6,7,9,43,52] The D1-D61N mutation retards the rates of S state transitions, which leads to slower O_2 release kinetics during the S_3 to S_0 transition.[40,50] The D1-D61N mutant also displays an extended lag phase and an increased miss factor, both similar to those of the D1-V185N mutation although the lag is longer and O_2 release is slower in D1-V185N.[36,39,40]

D1-Val185 is not immediately adjacent to D1-Asp61, and it has not been predicted to take part in the proton exit pathway; however, the substituted asparagine in the D1-V185N mutant could interact with the chloride ion ligated D2-K317 (Figure 1). A recent hypothesis concerning the function of this chloride ion argues that the ion prevents the formation of a salt bridge between D1-Asp61 and D2-Lys317, thus modulating the interactions between D1-Asp61 and both the substrate and the proton exit pathways of PSII.[43,53] It should be noted that the replacement of this chloride ion with iodide results in a decreased rate of O_2 release, an extended lag phase and a moderately increased miss factor, all to roughly the same extent as the D1-D61N and D1-V185N mutations.[41,54] It is therefore possible that the phenotypes of both mutants and the ion replacement are due to a similar interference in the interactions between D1-Asp61, the Mn_4CaO_5 cluster, and the chloride ion. It should also be noted that the H_2O molecules displaced by the D1-V185N mutation have been predicted to participate in proton transfer reactions in the S_2 to S_3 and S_3 to S_0 transitions in a model based on density functional theory (DFT) calculations.[55] Experimentally, measurements of flash-induced UV transients have convincingly demonstrated that chloride is essential for advancement through the S_2 to S_3 and S_3 to S_0 transitions, but not the S_1 to S_2 transition. However, the D1-V185N mutant PSII does advance through the higher S states albeit with a slightly elevated miss factor. Thus, if it does affect the chloride binding/activity, then it merely slows the process in which chloride is involved. Another possibility is that the

dx.doi.org/10.1021/bi400930g | *Biochemistry* 2013, 52, 6824−6833

mutation affects the mobility of water molecules due to the strong hydrogen bonding interaction presented by the amide moiety, especially between waters acting as hydrogen bond donors to the carbonyl functionality of the amide.[56] Considering that the native valine is hydrophobic, disallowing a polar interaction and thereby avoiding competition with the expected H-bond interactions among the adjacent water molecules facing the cluster, the mutational introduction of a strong, competing strong H-bonding functionality in the form of the amide of the D1-V185N substitution could disrupt the arrangement and dynamics of critical waters molecules.

Unlike the D1-V185T mutant, the D1-V185F mutant does not appear to have difficulty in assembling charge-separating PSII (Table 1). But despite being able to assemble PSII reaction centers at levels commensurate with wild-type *Synechocystis*, the D1-V185F strain is unable to evolve O_2. The Q_A reoxidation kinetics displayed in Figure 2 show that D1-V185F is able to form a stable charge separation, although with only 56% of the yield seen in wild-type *Synechocystis*. This suggests to us that the D1-V185F mutant is able to assemble at least some Mn clusters that exhibit charge recombination characteristics similar to wild-type clusters. It also provides evidence that D1-V185F may be able reach the S_2 state, assuming that the charge recombination similarities with the wild type indeed reflect oxidation of an assembled Mn_4CaO_5 cluster. Assuming that at least a fraction of the D1-V185F PSII centers contain a fully assembled Mn_4CaO_5 cluster, the most likely explanation for the inability of the D1-V185F mutant to evolve oxygen is an inability to complete either the S_2 to S_3 or the S_3 to S_0 transition.

The ability of the D1-V185F mutant to assemble PSII at near wild-type levels despite the large size difference between valine and phenylalanine suggests that the replaced residue occupies space previously occupied by H_2O rather than by other amino acids. In fact, basic modeling with PyMOL suggests that the least sterically hindered conformational isomer of the substitute phenylalanine residue causes it to displace H_2O molecules near Y_Z (Figure 1). One recent model of the water-oxidizing center (WOC) based on the 1.9 Å structure suggests that these H_2O molecules are part of a hydrogen bond network that facilitates the short hydrogen bond (2.46 Å) between Y_Z and His190.[10] The disruption of this hydrogen bond could have consequences for proton-coupled electron transport, which is vital for the efficiency of S state transitions; particularly in the higher S states. Other isomers of the substitute phenylalanine residue are of course possible and may lead to structural changes that affect first sphere ligands of the Mn_4CaO_5, especially D1-Gllu189. This does not rule out the possibility that the D1-V185F substitution interferes with the binding of the chloride co-factor, which is also known to prevent water oxidation.

Finally, it is thought that the lag phase associated prior to the re-reduction of Y_Z^{OX} and release of O_2 may be associated with the release of a proton.[47] Proton release kinetic experiments remain to be performed with the long lag phase mutants including D1-D61N and the mutant described here, D1-V185N. In principal, the release of a proton may be faster than the lag and the protracted lag phase in the mutant corresponds to some other molecular rearrangements. Comparison of the rate of proton release measured at high concentrations of indicator dye showed that a large (and pH dependent) fraction of proton release occurred faster than Y_Z^{OX} formation measured by UV spectroscopy.[57] This is consistent with the first of the two protons released during the $S_3 \rightarrow S_4 \Rightarrow S_0$ transition being ejected prior to a lag phase. For example, proton release upon Y_Z^{OX} formation may initiate a molecular rearrangement such as the movement of local water molecules involved in filling the opening coordination sites, which would be consistent with the inhibition of the lag phase seen in the D1-V185 mutants. In this context it is interesting that the nearest contact point of D1-V185 with the Mn cluster is O5, a bridging μ-oxo that is currently being discussed as altering its position and bonding during an isomerization of the oxo bridging pattern of the Mn_4CaO_5 cluster that could occur during the catalytic cycle.[58] The O5 oxo has also been tentatively assigned to the more slowly of the two exchangeable substrate water molecules.[59,60] Accordingly, we speculate that the D1-V185 mutations affect water exchange into this O5 location, thereby affecting both the movement of substrate water and, perhaps, an associated isomerization of the cluster. However, for both the D1-V185N and D1-V185F mutants, a definitive mechanistic link between amino acid substitution and the resulting phenotype cannot be assigned on the basis of the experiments presented here. Further experimentation will be needed to more clearly establish the cause of the defective oxygen evolution in these mutants, which may provide clues into the activity of the WOC.

■ ASSOCIATED CONTENT

Supporting Information

Description of the water cavity mutants not selected for further study, a table containing the values derived from the characterization of those strains, and a table of fitting parameters of fluorescence decay. This material is available free of charge via the Internet at http://pubs.acs.org.

■ AUTHOR INFORMATION

Corresponding Author

*R. L. Burnap. Phone: 405-744-7445. Fax: 405-744-6790. E-mail: rob.burnap@okstate.edu.

Funding

This work was funded by the National Science Foundation (MCB-1244586 to R.L.B.).

Notes

The authors declare no competing financial interest.

■ ACKNOWLEDGMENTS

Funding by the National Science Foundation MCB-1244586 (to R.L.B.) and the Edward R. & Mary M. Grula Distinguished Graduate Fellowship (to P.L.D.) is gratefully acknowledged.

■ ABBREVIATIONS:

CP43, chlorophyll protein subunit of the PSII complex encoded by the *psbC* gene; D1, reaction center protein encoded by the *psbA* gene; HEPES, 4-(2-hydroxyethyl)-1-piperazineethanesulfonic acid; HBG-11, BG-11 growth medium buffered with HEPES−NaOH pH 8; LED, light-emitting diode; Mn_4CaO_5, metal cluster functioning in H_2O oxidation; PSII, Photosystem II; WOC, H_2O oxidation complex of PSII; Y_Z, redox active tyrosine of the D1 protein acting as a secondary electron donor of the reaction center

■ REFERENCES

(1) Umena, Y., Kawakami, K., Shen, J. R., and Kamiya, N. (2011) Crystal structure of oxygen-evolving photosystem II at a resolution of 1.9 Ångstrom. *Nature 473*, 55−U65.

(2) Ferreira, K. N., Iverson, T. M., Maghlaoui, K., Barber, J., and Iwata, S. (2004) Architecture of the photosynthetic oxygen-evolving center. *Science 303*, 1831−1838.
(3) Kamiya, N., and Shen, J. R. (2003) Crystal structure of oxygen-evolving photosystem II from Thermosynechococcus vulcanus at 3.7-Å resolution. *Proc. Natl. Acad. Sci. U. S. A. 100*, 98−103.
(4) Loll, B., Kern, J., Saenger, W., Zouni, A., and Biesiadka, J. (2005) Towards complete cofactor arrangement in the 3.0 Å resolution structure of photosystem II. *Nature 438*, 1040−1044.
(5) Zouni, A., Witt, H. T., Kern, J., Fromme, P., Krauss, N., Saenger, W., and Orth, P. (2001) Crystal structure of photosystem II from *Synechococcus elongatus* at 3.8 Å resolution. *Nature 409*, 739−743.
(6) Murray, J. W., and Barber, J. (2007) Structural characteristics of channels and pathways in photosystem II including the identification of an oxygen channel. *J. Struct. Biol. 159*, 228−237.
(7) Ho, F. M., and Styring, S. (2008) Access channels and methanol binding site to the $CaMn_4$ cluster in Photosystem II based on solvent accessibility simulations, with implications for substrate water access. *Biochim. Biophys. Acta 1777*, 140−153.
(8) Vassiliev, S., Comte, P., Mahboob, A., and Bruce, D. (2010) Tracking the flow of water through photosystem II using molecular dynamics and streamline tracing. *Biochemistry 49*, 1873−1881.
(9) Ishikita, H., Saenger, W., Loll, B., Biesiadka, J., and Knapp, E. W. (2006) Energetics of a possible proton exit pathway for water oxidation in photosystem II. *Biochemistry 45*, 2063−2071.
(10) Saito, K., Shen, J.-R., Ishida, T., and Ishikita, H. (2011) Short Hydrogen Bond between Redox-Active Tyrosine YZ and D1-His190 in the Photosystem II Crystal Structure. *Biochemistry 50*, 9836−9844.
(11) Burnap, R., Koike, H., Sotiropoulou, G., Sherman, L. A., and Inoue, Y. (1989) Oxygen evolving membranes and particles from the transformable cyanobacterium *Synechocystis* sp. PCC6803. *Photosynth. Res. 22*, 123−130.
(12) Krishtalik, L. I., Tae, G. S., Cherepanov, D. A., and Cramer, W. A. (1993) The redox properties of cytochromes b imposed by the membrane electrostatic environment. *Biophys. J. 65*, 184−195.
(13) Qian, M., Dao, L., Debus, R. J., and Burnap, R. L. (1999) Impact of mutations within the putative Ca^{2+}-binding lumenal interhelical a-b loop of the photosystem II D1 protein on the kinetics of photoactivation and H_2O-oxidation in *Synechocystis* sp. PCC6803. *Biochemistry 38*, 6070−6081.
(14) Strickler, M. A., Walker, L. M., Hillier, W., and Debus, R. J. (2005) Evidence from biosynthetically incorporated strontium and FTIR difference spectroscopy that the C-terminus of the D1 polypeptide of photosystem II does not ligate calcium. *Biochemistry 44*, 8571−8577.
(15) Tang, X. S., and Diner, B. A. (1994) Biochemical and spectroscopic characterization of a new oxygen evolving photosystem II core complex from the cyanobacterium Synechocystis PCC 6803. *Biochemistry 33*, 4594−4603.
(16) Williams, J. G. K. (1988) Construction of specific mutations in Photosystem II photosynthetic reaction center by genetic engineering methods in *Synechocystis* 6803. *Methods Enzymol. 167*, 766−778.
(17) Debus, R. J., Barry, B. S., Sithole, I., Babcock, G. T., and McIntosh, L. (1988) Directed mutagenesis indicates that the donor to $P680^+$ in photosystem II is Tyr-161 of the D1 polypeptide. *Biochemistry 27*, 9071−9074.
(18) Debus, R. A., Nguyen, A. P., and Conway, A. B. (1990) Identification of ligands to manganese and calcium in photosystem II by site-directed mutagensis, in *Current Research in Photosynthesis* (Baltscheffsky, M., Ed.), pp 829−832, Kluwer, The Netherlands.
(19) Bricker, T. M., Morvant, J., Masri, N., Sutton, H. M., and Frankel, L. K. (1998) Isolation of a highly active photosystem II preparation from Synechocystis 6803 using a histidine-tagged mutant of CP 47. *Biochim. Biophys. Acta 1409*, 50−57.
(20) Li, Z., Bricker, T. M., and Burnap, R. (2000) Kinetic characterization of His-tagged CP47 photosystem II in Synechocystis sp. PCC6803. *Biochim. Biophys. Acta 1460*, 384−389.
(21) Burnap, R. L., Qian, M., and Pierce, C. (1996) The manganese-stabilizing protein (MSP) of photosystem II modifies the in vivo deactivation and photoactivation kinetics of the H2O-oxidation complex in Synechocystis sp. PCC6803. *Biochemistry 35*, 874−882.
(22) Meunier, P. C., Burnap, R. L., and Sherman, L. A. (1995) Modelling of the S state mechanism and Photosystem II manganese photoactivation in cyanobacteria. *Photosyn. Res. 47*, 61−76.
(23) Nixon, P. J., and Diner, B. A. (1992) Aspartate 170 of the photosystem II reaction center polypeptide D1 is involved in the assembly of the oxygen evolving manganese cluster. *Biochemistry 31*, 942−948.
(24) Hwang, H. J., Dilbeck, P., Debus, R. J., and Burnap, R. L. (2007) Mutation of arginine 357 of the CP43 protein of photosystem II severely impairs the catalytic S state cycle of the H2O oxidation complex. *Biochemistry 46*, 11987−11997.
(25) Allahverdiyeva, Y., Deak, Z., Szilard, A., Diner, B. A., Nixon, P. J., and Vass, I. (2004) The function of D1-H332 in Photosystem II electron transport studied by thermoluminescence and chlorophyll fluorescence in site-directed mutants of Synechocystis 6803. *Eur. J. Biochem. 271*, 3523−3532.
(26) Rappaport, F., Guergova-Kuras, M., Nixon, P. J., Diner, B. A., and Lavergne, J. (2002) Kinetics and Pathways of Charge Recombination in Photosystem II. *Biochemistry 41*, 8518−8527.
(27) Chu, H.-A., Nguyen, A. P., and Debus, R. A. (1994) Site-directed mutagenesis of photosynthetic oxygen evolution: Instability or inefficient assembly of the manganese cluster in vivo. *Biochemistry 33*, 6137−6149.
(28) Petrek, M., Otyepka, M., Banas, P., Kosinova, P., Koca, J., and Damborsky, J. (2006) CAVER: a new tool to explore routes from protein clefts, pockets and cavities. *Bmc Bioinf. 7*, 316.
(29) Diner, B. A., and Nixon, P. J. (1992) The rate of reduction of oxidized redox-active tyrosine, Z^+, by exogenous Mn^{2+} Is slowed in a site-directed mutant, at aspartate 170 of polypeptide D1 of photosystem II, inactive for photosynthetic oxygen evolution. *Biochim. Biophys. Acta 1101*, 134−138.
(30) Dau, H. (1994) Molecular Mechanisms and Quantitative Models of Variable Photosystem-Ii Fluorescence. *Photochem. Photobiol. 60*, 1−23.
(31) Butler, W. L., Visser, J. W. M., and Simons, H. L. (1973) The kinetics of light-induced changes of C-550, cytochrome b559 and fluorescence yield in chloroplasts at low temperature. *Biochim. Biophys. Acta, Bioenerg. 292*, 140−151.
(32) Vass, I., Kirilovsky, D., and Etienne, A. L. (1999) UV-B radiation-induced donor- and acceptor-side modifications of photosystem II in the cyanobacterium Synechocystis sp. PCC 6803. *Biochemistry 38*, 12786−12794.
(33) Chu, H. A., Nguyen, A. P., and Debus, R. J. (1995) Amino acid residues that influence the binding of manganese or calcium to photosystem II. 1. The lumenal interhelical domains of the D1 polypeptide. *Biochemistry 34*, 5839−5858.
(34) Chu, H.-A., Nguyen, A. P., and Debus, R. A. (1994) Site-directed mutagenesis of photosynthetic oxygen evolution: Increased binding or photooxidation of manganese in the absence of the extrinsic 33-kDa polypeptide in vivo. *Biochemistry 33*, 6150−6157.
(35) Chu, H. A., Nguyen, A. P., and Debus, R. J. (1995) Amino acid residues that influence the binding of manganese or calcium to photosystem II. 2. The carboxy terminal domain of the D1 polypeptide. *Biochemistry 3496*, 5859−5882.
(36) Dilbeck, P. L., Hwang, H. J., Zaharieva, I., Gerencser, L., Dau, H., and Burnap, R. L. (2012) The D1-D61N mutation in *Synechocystis* sp PCC 6803 allows the observation of pH-sensitive intermediates in the formation and release of O_2 from Photosystem II. *Biochemistry 51*, 1079−1091.
(37) Lavorel, J. (1976) Matrix analysis of the oxygen evolving system of photosynthesis. *J. Theor. Biol. 57*, 171−185.
(38) Jursinic, P. A., and Dennenberg, R. J. (1990) Oxygen release time in leaf discs and thylakoids of peas and Photosystem II membrane fragments of Spinach. *Biochim. Biophys. Acta 1020*, 195−206.
(39) Clausen, J., Debus, R. J., and Junge, W. (2004) Time-resolved oxygen production by PSII: Chasing chemical intermediates. *Biochim. Biophys. Acta 1655*, 184−194.

(40) Hundelt, M., Hays, A. M., Debus, R. J., and Junge, W. (1998) Oxygenic photosystem II: the mutation D1-D61N in *Synechocystis* sp. PCC 6803 retards S state transitions without affecting electron transfer from Y_Z to $P680^+$. *Biochemistry 37*, 14450−14456.
(41) Boussac, A., Ishida, N., Sugiura, M., and Rappaport, F. (2012) Probing the role of chloride in Photosystem II from *Thermosynechococcus elongatus* by exchanging chloride for iodide. *Biochim. Biophys. Acta 1817*, 802−810.
(42) Pokhrel, R., Service, R. J., Debus, R. J., and Brudvig, G. W. (2013) Mutation of Lysine 317 in the D2 Subunit of Photosystem II Alters Chloride Binding and Proton Transport. *Biochemistry 52*, 4758−4773.
(43) Rivalta, I., Amin, M., Luber, S., Vassiliev, S., Pokhrel, R., Umena, Y., Kawakami, K., Shen, J. R., Kamiya, N., Bruce, D., Brudvig, G. W., Gunner, M. R., and Batista, V. S. (2011) Structural-functional role of chloride in photosystem II. *Biochemistry 50*, 6312−6315.
(44) Vassiliev, S., Zaraiskaya, T., and Bruce, D. (2012) Exploring the energetics of water permeation in photosystem II by multiple steered molecular dynamics simulations. *Biochim. Biophys. Acta 1817*, 1671−1678.
(45) Gerencser, L., and Dau, H. (2010) Water oxidation by photosystem II: H_2O-D_2O exchange and the influence of pH support formation of an intermediate by removal of a proton before dioxygen creation. *Biochemistry 49*, 10098−10106.
(46) Haumann, M., Liebisch, P., Muller, C., Barra, M., Grabolle, M., and Dau, H. (2005) Photosynthetic O_2 formation tracked by time-resolved X-ray experiments. *Science 310*, 1019−1021.
(47) Rappaport, F., Lavergne, J., and Blanchard-Desce, M. (1994) Kinetics of electron transfer and electrochromic change during the redox transitions of the photosynthetic oxygen-evolving complex. *Biochim. Biophys. Acta 1184*, 178−192.
(48) Haumann, M., Bogershausen, O., Cherepanov, D., Ahlbrink, R., and Junge, W. (1997) Photosynthetic oxygen evolution: H/D isotope effects and the coupling between electron and proton transfer during the redox reactions at the oxidizing side of Photosystem II. *Photosyn. Res. 51*, 193−208.
(49) Koike, H., Hanssum, B., Inoue, Y., and Renger, G. (1987) Temperature dependence of the S state transitions in a thermophilic cyanobacterium, *Synechococcus vulcanus* Copeland measured by absorption changes in the ultraviolet region. *Biochim. Biophys. Acta 893*, 524−533.
(50) Hundelt, M., Hays, A. M. A., Debus, R. J., and Junge, W. (1998) The mutation D1-D61N in PS II of *Synechocystis*: Retardation of ET from OEC->Y_z^{ox} and no effect on Y_z->$P680^+$, in *Photosynthesis: Mechanisms and Effects* (Garab, G., Ed.), pp 1387−1390, Kluwer Academic Publishers, The Netherlands.
(51) Kawakami, K., Umena, Y., Kamiya, N., and Shen, J. R. (2011) Structure of the catalytic, inorganic core of oxygen-evolving photosystem II at 1.9 Å resolution. *J. Photochem. Photobiol., B 104*, 9−18.
(52) Sproviero, E. M., Gascon, J. A., McEvoy, J. P., Brudvig, G. W., and Batista, V. S. (2008) Quantum mechanics/molecular mechanics study of the catalytic cycle of water splitting in photosystem II. *J. Am. Chem. Soc. 130*, 3428−3442.
(53) Pokhrel, R., McConnell, I. L., and Brudvig, G. W. (2011) Chloride regulation of enzyme turnover: application to the role of chloride in photosystem II. *Biochemistry 50*, 2725−2734.
(54) Wincencjusz, H., Yocum, C. F., and van Gorkom, H. J. (1999) Activating anions that replace Cl- in the O2-evolving complex of photosystem II slow the kinetics of the terminal step in water oxidation and destabilize the S_2 and S_3 states. *Biochemistry 38*, 3719−3725.
(55) Siegbahn, P. E. M. (2012) Mechanisms for proton release during water oxidation in the S_{-2} to S_{-3} and S_{-3} to S_{-4} transitions in photosystem II. *Phys. Chem. Chem. Phys. 14*, 4849−4856.
(56) Dixon, D. A., Dobbs, K. D., and Valentini, J. J. (1994) Amide-Water and Amide-Amide Hydrogen Bond Strengths. *J. Phys. Chem. 98*, 13435−13439.
(57) Haumann, M., and Junge, W. (1994) Extent and rate of proton release by photosynthetic water oxidation in thylakoids - Electrostatic relaxation versus chemical production. *Biochemistry 33*, 864−872.
(58) Pantazis, D. A., Ames, W., Cox, N., Lubitz, W., and Neese, F. (2012) Two interconvertible structures that explain the spectroscopic properties of the oxygen-evolving complex of photosystem II in the S2 state. *Angew. Chem., Int. Ed. Engl. 51*, 9935−9940.
(59) Cox, N., and Messinger, J. (2013) Reflections on substrate water and dioxygen formation. *Biochim. Biophys. Acta 1827*, 1020−1030.
(60) Hillier, W., and Wydrzynski, T. (2008) ^{18}O-Water exchange in photosystem II: Substrate binding and intermediates of the water splitting cycle. *Coord. Chem. Rev. 252*, 306−317.